ChemSusChem

Research Article
doi.org/10.1002/cssc.202301300

Chemistry Europe
European Chemical Societies Publishing

www.chemsuschem.org

Special Collection

Electrochemical Sodium Storage in Hard Carbon Powder Electrodes Implemented in an Improved Cell Assembly: Insights from In-Situ and Ex-Situ Solid-State NMR

Edina Šić,[a] Konstantin Schutjajew,[b] Ulrich Haagen,[b] Hergen Breitzke,[a] Martin Oschatz,[b, c] Gerd Buntkowsky,*[a] and Torsten Gutmann*[a]

In this work, we report on an improved cell assembly of cylindrical electrochemical cells for ^{23}Na *in-situ* solid-state NMR (ssNMR) investigations. The cell set-up is suitable for using powder electrode materials. Reproducibility of our cell assembly is analyzed by preparing two cells containing hard carbon (HC) powder as working electrode and sodium metal as reference electrode. Electrochemical storage properties of HC powder electrode derived from carbonization of sustainable cellulose are studied by ssNMR. ^{23}Na *in-situ ss*NMR monitors the sodiation/desodiation of a Na|$NaPF_6$|HC cell (cell **1**) over a period of 22 days, showing high cell stability. After the galvanostatic process, the HC powder material is investigated by high resolution ^{23}Na *ex-situ* MAS NMR. The formation of ionic sodium species in different chemical environments is obtained. Subsequently, a second Na|$NaPF_6$|HC cell (cell **2**) is sodiated for 11 days achieving a capacity of 220 mAh/g. ^{23}Na *ex-situ* MAS NMR measurements of the HC powder material extracted from this cell clearly indicate the presence of quasi-metallic sodium species next to ionic sodium species. This observation of quasi-metallic sodium species is discussed in terms of the achieved capacity of the cell as well as of side reactions of sodium in this electrode material.

Introduction

The rapid growth of the global energy consumption has raised societies' awareness of the necessity to utilize novel concepts to compromise the worldwide energy demands.[1] Renewable as well as sustainable energy sources associated with facile accessibility, low-cost and environmentally benign manufacturing are regarded and promoted as solution for the ongoing energy transition.[2] To fulfil the need to store large amounts of this energy, progress has been made in the advancement of sodium/sodium-ion battery technologies as a potential replacement for lithium-based electrochemical storage systems.[3] Implementation of lithium-ion batteries might become limited due to global supply shortage of lithium resources and the estimated rising price at the market.[4,5] On the contrary, sodium-based technology relies on cheap and worldwide abundant raw materials.[6] Considering in particular applications in the field of mobility and high-end consumer devices, sodium-ion battery systems, however, suffer from significantly lower energy density as compared to the established lithium-based technologies.[7] Thus, recent attention has especially been paid to the design of novel electrode materials that contribute to the development of next-generation sodium-based systems with improved energy density.[8] In particular, disordered carbon materials such as hard carbon (HC) that can be manufactured from low-cost and eco-friendly renewable sources such as cellulose have been proposed as attractive anode material in sodium-ion batteries.[9,10] Significant efforts have been devoted to the optimization of their structures for sodium storage resulting in high reversible capacity up to 300 mAh/g,[11] good electronic conductivity,[12] low operating potential down to 0 V vs. Na/Na^+[13] and high cycling stability.[14] These previous research achievements in the field of sodium-ion technology promote its further development as well as its spread for energy storage applications. In this context, further targeted improvement of HC electrodes requires a detailed understanding of the fundamental (electro)chemical mechanisms of the sodium storage within the various structure motives of the carbon material.

Detailed knowledge of the sodium storage inside the material during sodiation/desodiation processes on the atomic

[a] E. Šić, Dr. H. Breitzke, Prof. G. Buntkowsky, Prof. T. Gutmann
Eduard Zintl Institute for Inorganic and Physical Chemistry
Technical University of Darmstadt
Peter-Grünberg-Straße 8, 64287 Darmstadt (Germany)
E-mail: gerd.buntkowsky@chemie.tu-darmstadt.de
gutmann@chemie.tu-darmstadt.de

[b] Dr. K. Schutjajew, U. Haagen, Prof. M. Oschatz
Institute for Technical Chemistry and Environmental Chemistry
Friedrich-Schiller-University Jena
Philosophenweg 7a, 07743 Jena (Germany)

[c] Prof. M. Oschatz
Center for Energy and Environmental Chemistry Jena (CEEC Jena)
Friedrich Schiller University Jena
Philosophenweg 7a, 07743 Jena (Germany)

Supporting information for this article is available on the WWW under https://doi.org/10.1002/cssc.202301300

Special Collection This publication is part of a joint Special Collection of ChemSusChem, Batteries & Supercaps, and Energy Technology including invited contributions focusing on the "International Conference on Sodium Batteries (ICNaB)". Please visit chemsuschem.org/collections to view all contributions.

level is crucial for an optimized cell design. This necessitates the application of specific analytic techniques, which can observe these processes for sodium in disordered environments on the micro- and nanoscopic level. ^{23}Na *in-situ* solid-state NMR spectroscopy (ssNMR) is a valuable characterization technique which enables to monitor sodium ion transport, electrochemical degradation processes as well as sodium ion/metal storage during the charging/discharging of an active cell as shown in the literature.[6,15–20]

In contrast to the previous works referred to above, electrochemical processes in an active Na|$NaPF_6$|HC cell occurring during galvanostatic cycling are investigated in the present study using an adapted cell design and improved cell assembly for ^{23}Na *in-situ* ssNMR. This cell design is derived from the cylindrical one for *in-situ* ssNMR which has been introduced and tested for a Cu_3P/Li battery by Poli et al.[21] Such design offers several advantages compared to the flat cell design used for *in-situ* NMR studies of C/Li cells[22] or formerly by some of the authors for studying Na|$NaPF_6$|SiCN cells.[15] (i) HC can be used as powder to form the electrode in the cell assembly, which enables to employ a much larger amount of electrode material compared to flat cell designs. This increased amount of electrode material leads to more total electrochemical conversion and thus higher sensitivity in the NMR experiments towards the species of interest. (ii) The electrode material can be applied directly in the cell without conductive additives and binder, and thus influences or background signals from such compounds on the NMR signals can be ruled out. In other words, the NMR observations will surely only originate from sodium species either in the metallic electrode, in the electrolyte, or in the hard carbon. (iii) There is a lower risk for electrolyte loss or decomposition caused by solvent leakage or penetration of oxygen/moisture through the cell parts, respectively, and (iv) the cell-design of so-called "Swagelok cells" often used in academic laboratory-scale battery research is mimicked in a better way.

In this work, two electrochemical Na|$NaPF_6$|HC cells are prepared by an improved cell assembly for *in-situ* ssNMR. Using this cell assembly to set up a cell composed of sodium metal and a HC powder electrode is essential to have an electrochemically active system with high cell stability and reproducible sodiation profile. Applying ^{23}Na *in-situ* ssNMR, changes of the local surrounding of sodium nuclei within both cells are monitored and discussed during the electrochemical processes. First a Na|$NaPF_6$|HC cell (cell **1**) was cycled for 22 days including two sodiation cycles and one desodiation cycle. After the second sodiation cycle, cell **1** reached a capacity of ca. 160 mAh/g. To monitor the sodium storage inside the HC powder electrode more in detail, a second Na|$NaPF_6$|HC cell (cell **2**) was fully sodiated for 11 days at higher current from the beginning of the experiment, reaching a higher capacity of 220 mAh/g. The sodium storage in this cell **2** is studied by ^{23}Na *ex-situ* ssNMR of the HC electrode extracted after sodiation and discussed in terms of capacity and side reactions.

Results and Discussion

Structural characterization and sodium storage properties of the HC material

Before the NMR investigations, the structural and electrochemical properties of the HC powder material derived from microcrystalline cellulose have been analysed. The XRD pattern is shown in Figure S1. The HC demonstrates the typical characteristics of a primarily disordered graphitic carbon with broad reflections centered at 2Θ of 22° and 44° in the diffraction pattern, representing the (002) and (100) reticular planes of graphite, respectively. N_2 adsorption was carried out to analyse the specific surface area (SSA) and the total pore volume (V_t) accessible for nitrogen. HC shows a low BET SSA of 3 $m^2 g^{-1}$ and low V_t of 0.003 $cm^3 g^{-1}$. According to the IUPAC classification, [23] an infinite growth at $p/p_0 = 1$ defines a type II isotherm which is visible in Figure S2. It can thus be summarized that, the material provides a structure typical for HC materials with small graphitic domains and a low SSA which is a good fundament for sodium ion storage between slightly expanded graphitic carbon layers and in closed small pores not detectable by nitrogen adsorption as it was already shown in the work of Ghimbeu et al.[24] For more details on the electrochemistry the interested reader is referred to ESI Figure S3, where the first and sixth sodiation and desodiation cycles of a Swagelok-type cell containing HC with binder are shown at a current of 20 mAh/g.

^{23}Na in-situ solid-state NMR

The cycling profile of the prepared Na|$NaPF_6$|HC cell (cell **1**) and an enlarged 3D view of the ^{23}Na *in-situ* ssNMR spectra in the chemical shift range between −30 and 10 ppm as well as between 1120 and 1150 ppm corresponding to the typical regions of ionic sodium and metallic sodium, respectively, are presented in Figure 1a–c. The whole spectral range of the ^{23}Na *in-situ* ssNMR spectra is provided in ESI in Figure S4. The ^{23}Na *in-situ* NMR spectra in Figure 1a-b show a broad resonance at −8.5 ppm. This signal at −8.5 ppm is attributed to sodium ions in the $NaPF_6$ electrolyte solution and shows significant changes in its intensity depending on the applied voltage.[19] Furthermore, negligible changes in chemical shift and line width of the signal at −8.5 are obtained as visible by comparing slices of the ^{23}Na *in-situ* ssNMR (see ESI in Figure S5). During the first hour of HC sodiation to ca. 1.4 V vs. Na^+/Na, the signal rises in intensity indicating sodium ion transport from the sodium metal electrode to the HC powder electrode. Subsequently, the signal intensity decreases up to 1.3 V and returns when achieving the lower cut-off voltage of 2 mV. On the contrary, the signal intensity decreases when the voltage changes to 2.5 V indicating sodium ion transport back to the sodium metal electrode. Hereby, small intensity fluctuations are noticed before reaching the highest voltage (2.5 V) as well as during the sodiation of the cell. These changes in intensity of the signal at −8.5 ppm are an indication for undesired reactions of $NaPF_6$ with the solvents

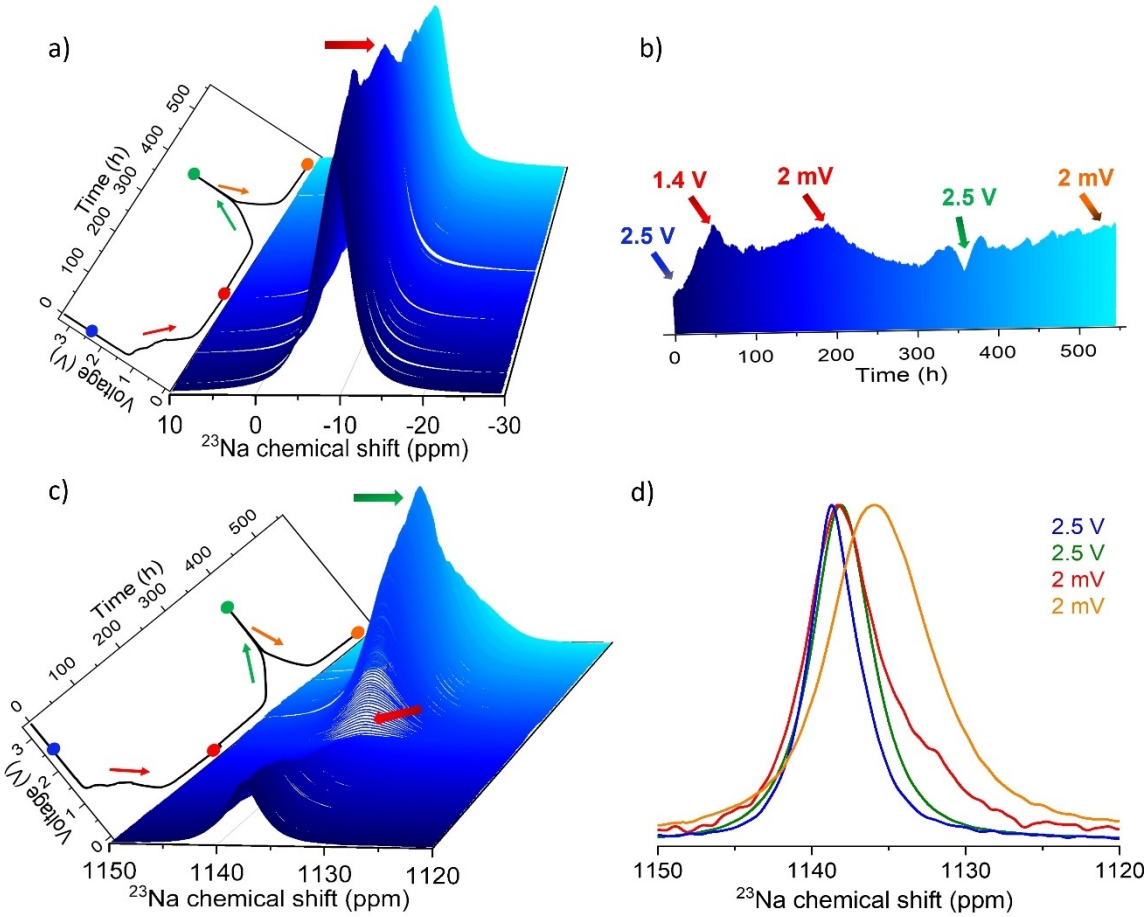

Figure 1. a) Enlarged 3D view of the ^{23}Na *in-situ* NMR spectra in the range between 10 and −30 ppm obtained for the Na|$NaPF_6$|HC cell (cell **1**). b) Projection of the enlarged 3D view of the ^{23}Na *in-situ* NMR spectra (a) illustrating the intensity fluctuations during sodiation/desodiation of cell. c) Enlarged 3D view of the ^{23}Na *in-situ* NMR spectra in the range between 1150 and 1120 ppm showing intensity changes during electrochemical cycling. d) Extracted and normalized ^{23}Na *in-situ* NMR spectra in the range between 1150 and 1120 ppm at the initial state of charge at ca. 2.5 V, and at the highest and at the lowest voltage of 2.5 V and 2 mV to illustrate changes in line shape. Note: The green and red arrows in the ^{23}Na *in-situ* NMR spectra of cell **1** indicate signal maxima and minima depending on the state of the charge.

that cause degradation/decomposition to several site products on the surface of the electrodes leading to the formation of a solid electrolyte interface (SEI), especially, since these processes do not seem to reoccur during the subsequent sodiation cycle. Besides, the changes obtained in the spectral range between −30 and 10 ppm of the ^{23}Na *in-situ* ssNMR spectra suggest the insertion of sodium ions inside of the HC powder electrode. Such process has been also reported in previous studies by Stratford and Gotoh and co-workers. [17,18] The relatively large line widths of the signals in ^{23}Na *in-situ* ssNMR spectra, caused by bulk magnetic susceptibility, quadrupolar interactions, static conditions and the disordered structures complicate their interpretation and make it challenging to distinguish sodium ion environments.

In Figure 1c, a signal is visible at 1138 ppm which is assigned to metallic sodium. This signal shows qualitatively opposite changes in intensity compared to the signal of the electrolyte at −8.5 ppm (Figure 1a,b). The signal at 1138 ppm drops down significantly in intensity with decreasing voltage, whereas a continuous growth is noticed at increasing voltage. This observation clearly illustrates that sodium is exchanged between the sodium metal electrode and the HC powder electrode across the electrolyte solution.

Comparing the normalized ^{23}Na *in-situ* ssNMR spectra in the region between 1120 and 1150 ppm extracted at the beginning of the cell cycling and at the lowest cut-off voltage of 2 mV (Figure 1d), changes in the line shape are observed. In the ^{23}Na *in-situ* NMR spectrum recorded at 2 mV (see Figure 1d, red spectrum) an additional signal at ca. 1132 ppm becomes visible as a shoulder. Interestingly, the spectrum recorded at the highest cell voltage of 2.5 V (see Figure 1d, green spectrum) shows that this shoulder peak has disappeared. During the second sodiation cycle to 2 mV, the sodium metal region has been shifted about 2 ppm to higher field and becomes remarkably broadened, so that the signal attributed to the sodium counter electrode and the shoulder peak cannot be distinguished (see Figure 1d, orange spectrum). The changes in signal intensity, line broadening and the spectra shapes suggest the formation and growth of deposited sodium structures which differ in structure from the initial ones. Similar observations on formed metallic micro- and nano-structures have been also described in the literature. [15,18] Here, it has to be noticed

that the signal intensity in the ^{23}Na *in-situ* ssNMR spectra is strongly influenced by the skin depth effect (see ESI for details).

It has to be mentioned that cell **1** shows irreversible capacity losses (see ESI Figure S6a) during galvanostatic cycling. After the first sodiation cycle a capacity of 206 mAh/g is obtained, whereas the capacity drops down to ca. 160 mAh/g after the second cycle. This decrease of capacity is most probably related to the formation of the solid-electrolyte-interphase (SEI).

To investigate the sodium storage in HC powder electrodes at higher capacity, a second Na|$NaPF_6$|HC electrochemical cell (cell **2**) was prepared similar to cell **1** and the HC has been fully sodiated once. The voltage profile and capacity curve of cell **2** are presented in ESI in Figure S6b. Cell **2** reaches the lowest voltage after ca. 9 days of sodiation resulting in a capacity of approximately 200 mAh/g which is comparable with cell **1** after the first sodiation cycle at overall comparable current. This clearly indicates the reproducibility of our cell assembly.

The ^{23}Na *in-situ* NMR spectra of the Na|$NaPF_6$|HC cell **2** are displayed in ESI in Figure S7. Since these spectra show similar changes in intensity and broadening of the signals compared to cell **1** they are not discussed in more detail here.

^{23}Na ex-situ solid-state NMR

Since the *in-situ* data presented in the previous section do not provide enough resolution to identify different types of sodium species, the prepared cells were disassembled after galvanostatic cycling and the hard carbon material was inspected by ^{23}Na *ex-situ* solid-state NMR.

After 22 days of galvanostatic cycling, cell **1** with a capacity of ca. 160 mAh/g was disassembled, and the washed HC powder electrode was investigated by high resolution ^{23}Na *ex-situ* MAS ssNMR. In the ^{23}Na *ex-situ* MAS NMR spectrum of the HC electrode material, resonances in the spectral region of metallic sodium between 1120 and 1150 ppm are not visible (spectral range not shown). In the spectral region between 50 and −50 ppm presented in Figure 2a broad overlapping resonances are observed attributed to ionic sodium species. This spectral range can be deconvoluted into four Gaussian/Lorentzian lines with centers at −11.6, −7.5, 5.7 and 12.8 ppm. The sharp signal at −11.6 ppm is attributed to traces of sodium ions originating from the electrolyte solution.[25] The resonance at 5.7 ppm is assigned to the irreversible formation of sodium salts such as NaF at the surface of the HC electrode caused by electrolyte decomposition. The presence of NaF is underlined by the ^{19}F *ex-situ* MAS NMR spectrum shown in ESI Figure S8, where a signal at −225 ppm typical for NaF is obtained.[15,26] Goward and co-workers as well as some of the authors of the present study have previously revealed the formation of NaF in Na/Na^+ by ^{23}Na MAS NMR and ^{19}F MAS NMR.[5,15] The broad resonances at 12.8 and −7.5 ppm are tentatively assigned to sodium ions stored inside of carbon layers and pores. This assignment is based on the large line widths (full width at half maximum) of these signals (21.95 ppm and 11.15 ppm corresponds to 3485 and 1770 Hz, respectively) which indicate high-disordered local environments around sodium nuclei and/or restricted mobility.[27,28] Similar observations have been made by Gotoh et al.[25] who studied the storage properties of HC materials depending on carbonization temperature. According to Gotoh et al.[25,29] and Kim et al.[30] the resonances in the chemical shift region between 30 and −60 ppm are attributed to sodium ions in electrolyte, SEI compounds as well as to sodium ions intercalated between graphene layers or stored in closed pores. These findings are also in excellent agreement with operando ^{23}Na magnetic resonance imaging studies by Britton et al.[20]

The ^{23}Na *ex-situ* MAS NMR spectrum of the non-washed HC powder electrode extracted from cell **2** at a capacity of 220 mAh/g after full sodiation to 2 mV (11 days of sodiation) is presented in Figure 2b. Resonances in the chemical shift range between 30 and −40 ppm are observed. The spectrum pattern can be deconvoluted into three Gaussian/Lorentzian lines at −11.6, −7.5 and 5.7 ppm. These signals are attributed to sodium ions in the electrolyte, sodium ions stored inside of HC, and sodium ions in NaF, respectively. In addition, a broad peak at 840 ppm appears in the ^{23}Na *ex-situ* MAS NMR spectrum, which is not visible in ^{23}Na *in-situ* NMR spectra most probably due to line broadening caused by second order quadrupolar coupling and bulk magnetic susceptibility effect.[15,18] Note, that the ^{23}Na *in-situ* NMR spectra are recorded at 7 T, whereas the ^{23}Na *ex-situ* MAS NMR measurements are performed at higher magnetic field of 14.1 T. At higher magnetic fields, the second order quadrupolar broadening is reduced significantly leading to narrower signals in spectra. The impact of magnetic field strength on line broadening in spectra caused by quadrupolar interactions has been studied in more details in our previous work. [15] This signal at 840 ppm clearly indicates the presence of quasi-metallic sodium clusters formed in the HC powder electrode. Similar observations have been reported in refs. .[10,16–18,20,25,27] Interestingly, this signal referring to quasi-metallic sodium clusters has not been observed for the HC material extracted from cell **1**. A reasonable explanation is the sodiation time that correlates with the cell capacity, and which was 2 days longer for cell **2** compared to cell **1** leading to the formation of larger amounts of quasi-metallic sodium clusters.

Surprisingly, the signal at 840 ppm has disappeared when the sample is spun at a higher frequency of 15 kHz as shown in Figure 2c. Quasi-metallic sodium tends to decompose during the storage period/time of the cycled HC powder material after extracting from the cell. Oxidation of metallic cluster is caused by traces of moisture/oxygen and favored by heat input, which is initialized by the sample spinning. The presence of side reactions is underlined by the line shape of the resonances in the chemical shift region between 30 and −40 ppm, which has significantly changed in the spectrum recorded at 15 kHz (Figure 2c) compared to the spectrum recorded at 10 kHz (Figure 2b). Performing a deconvolution of the spectrum obtained at 15 kHz, four Gaussian/Lorentzian lines with centers at −11.6, −7.5, −6.0 and 5.7 ppm are identified. The increased intensity of the signal at 5.7 ppm in the 15 kHz spectrum (Figure 2c) compared to the 10 kHz spectrum (Figure 2b) suggests an increased formation of NaF due to reaction of the

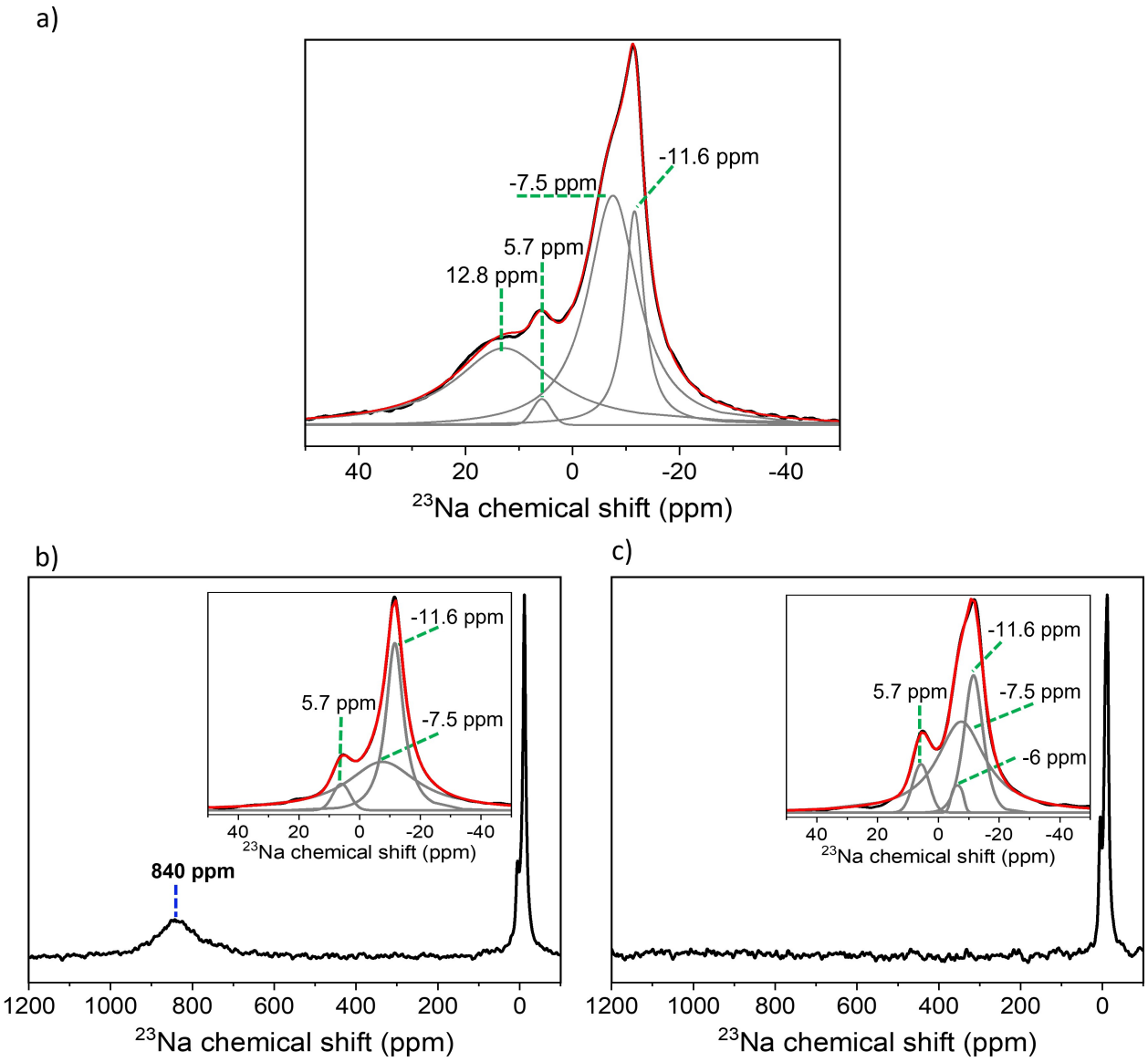

Figure 2. a) ^{23}Na *ex-situ* MAS NMR spectrum in the range between 50 and −50 ppm of the HC powder electrode material of cell **1** after galvanostatic cycling for 22 days. The spectrum was measured at 14 T and 15 kHz spinning. b) ^{23}Na *ex-situ* MAS NMR spectrum in the region between 1200 and −100 ppm of the HC powder electrode material of cell **2** after sodiation for 11 days. The spectrum was measured at 14 T and 10 kHz spinning. c) ^{23}Na *ex-situ* MAS NMR spectrum of the HC powder electrode material of cell **2** after sodiation for 11 days. The spectrum was measured at 14 T and 15 kHz spinning. Note: experimental spectra are presented as black curves. Spectral deconvolutions employing three or four Gaussian/Lorentzian lines are illustrated as grey curves and cumulative signals as red curves.

pristine quasi-metallic sodium clusters with traces of the electrolyte solution. The broadening of the signal at −7.5 ppm traces back to an increased structural disorder in the local environment of sodium nuclei after side reaction. An increased structural disorder affects the spectrum shape in different ways. (i) An asymmetric surrounding of sodium yields to a larger distribution of isotropic chemical shifts. (ii) Quadrupolar interactions can become significantly larger when the symmetry of the sodium environment decreases. Both lead to a broadening of signals in spectra and effects of the second order quadrupolar interaction may distort the spectral shape. Such distortion is not necessarily considered sufficiently by Gaussian/Lorentz lines. To exclude second order quadrupole contribution, ultra-high field ssNMR measurements or multiple quantum magic angle spinning (MQMAS) NMR experiments are required which are beyond the scope of this work. Although, from the obtained results the origin for the absence of a signal attributed to quasi-metallic sodium cannot be fully explained, it is considered as secured that unwanted side reaction play a crucial role.

Conclusions

Significant progress in investigation of powder electrodes for sodium-based batteries has been made applying ^{23}Na *in-situ*

and *ex-situ* ssNMR studies. For the first time, HC powder material manufactured by carbonization of sustainable as well renewable cellulose has been used to prepare sodium/sodium ions cells with long cell stability for ^{23}Na *in-situ* ssNMR studies. By assembling a Na|$NaPF_6$|HC cells as described in the experimental section, homogenous and tight packing of cell components is ensured. This packing provides enough pressure and sufficient electrical contact between the HC material und Cu-foil collector for cell stability for minimum 22 days. Intensity changes of the signals in the *in-situ* ssNMR spectra allow to monitor changes of the chemical environment of sodium during the cell cycling. Signal broadening caused by quadrupolar interactions and effect of bulk magnetic susceptibility, however, makes it difficult to observe sodium metal clusters in ^{23}Na *in-situ* ssNMR. *Ex-situ* ssNMR studies of the HC after disassembling of the cycled cell help to identify the formation of quasi-metallic sodium clusters in the HC material. The cell disassembly has to be performed with care under inert conditions and has to take place immediately after stopping the electrochemical process as quasi-metallic sodium species strongly tend to decompose. Oxidizing conditions as well as heat input induced by MAS in *ex-situ* ssNMR experiments may favor unwanted reactions in the system. These important conclusions have to be taken into account when investigating quasi-metallic sodium clusters in powder electrode materials by *in-situ* and ex-situ ssNMR in future.

Experimental Section

Materials synthesis and characterization

The HC material for both cells was prepared following the synthesis protocol of Ghimbeu et al.[24] Microcrystalline cellulose (Sigma-Aldrich) was treated in a two-step pyrolysis procedure. Both heat treatments were performed under nitrogen atmosphere in horizontal tube furnaces. In the first step, cellulose was heated to 200 °C at a heating rate of 20 °C/min followed by a slow heating rate of 1 °C/min up to 450 °C. Then, the sample was cooled down to room temperature. In the second step, the as-prepared material was transferred to a high-temperature horizontal tube furnace and subjected to a further heat treatment at 1500 °C for 60 min with a ramp of 3.3 °C/min. No conductive compounds or binder materials have been added to this HC power before using it for preparation of electrochemical cells for the NMR experiments.

Powder X-ray diffraction (XRD) patterns of the HC material were recorded on a Bruker D2 PHASER in Bragg-Brentano geometry in a 2Θ range of 10–80° with a resolution of 0.02° and 3 s per step with $Cu_{K\alpha}$ radiation ($\lambda = 0.154$ nm) and a Si-strip detector with 160 channels and a position sensitive detector opening of 2°. The samples were placed on a horizontal silicon single crystal holder.

Gas adsorption measurements were conducted on a Quadrasorb SI by Quantachrome Instruments. N_2 at its condensation point (−196 °C) was used as probe gas. The sample was degassed under vacuum at 120 °C for at least 20 h before each measurement. The total pore volume was determined at a relative pressure of $p/p_0 = 0.95$. The specific surface area (SSA) of the materials was calculated from the adsorption branch by using the Brunauer-Emmett-Teller (BET) model in the relative pressure range $p/p_0 = 0.05–0.20$.

Electrochemical cell setup and cycling

Poli et al.[21] proposed a new cell design with cylindrical geometry for *in-situ* ssNMR investigations. This design contains a robust plastic housing with an outer diameter of 10 mm that is suitable for the charging/discharging of a Cu_3P/CB cell containing a carbon black (CB) powder electrode for lithium-ion studies. In the present study, we used such a cylindrical cell design for ^{23}Na *in-situ* ssNMR investigations of the sodiation/desodiation processes of a Na|$NaPF_6$|HC cell containing HC powder as electrode. A schematic illustration of the used cell for the ^{23}Na *in-situ* ssNMR studies of Na|$NaPF_6$|HC is shown in Figure 3. A cell with an outer diameter of 15 mm was used to ease the assembling and handling. This electrochemical cell consists of two separable parts, a cylindrical capsule and a cap made from polypropylene. The cell preparation was performed in a glove box under Argon atmosphere. During the cell assembly, both the water and oxygen level were below 3 ppm. A small piece (7 mg) of metallic sodium (Sigma-Aldrich) was placed at the bottom of the cell capsule and connected to an Ag/Cu wire. Subsequently, borosilicate glass fiber sheets (Ahlstrom-Munksjö) dried in vacuum at 80° were placed on the metallic sodium and soaked with ca. 100 µl of 1 M $NaPF_6$ in ethylene carbonate and diethyl carbonate (EC:DEC 3:7 volume ratio with 5 wt% of fluoroethylene carbonate additive, Xiamen Tob New Energy Technology Co., Ltd) as electrolyte solution. On top of the separator, 30 mg of HC powder were inserted. A homogeneous compact packing of the cell was reached by adding a small amount of the powder sample inside of the capsule and gradually compressing it. This process was repeated several times until the cell capsule was filled to a certain height providing still enough space for closing with the cap. In addition, another 100 µL of 1 M $NaPF_6$ was distributed over the powder electrode. The cell was sealed by screwing a cap, on which copper mesh as current collector was supported that was

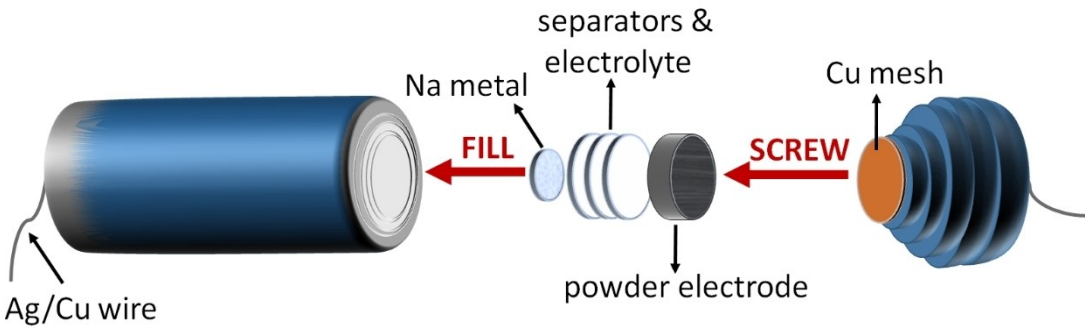

Figure 3. Schematic illustration of the cylindrical cell design proposed by Poli at al.[21] adapted for ^{23}Na *in-situ* NMR studies of a Na|$NaPF_6$|HC cell. Contrary to Poli et. al the feeding of the cell was performed in an inversed order.

connected to an Ag/Cu wire for electrical contact to the powder electrode. The closed cell was wrapped with a Parafilm foil (Sigma-Aldrich) resulting in a well-sealed system for *in-situ* ssNMR studies.

The first prepared Na|$NaPF_6$|HC cell (cell **1**) was cycled on a Bio-Logic SP-150 potentiostat using the EC-Lab software version 11.40 applying galvanostatic cycling with potential limitation. The HC was sodiated/desodiated in a voltage window between 2 mV and 2.5 V for 22 days. The cell cycling was started applying a low current of 15 μA. After 70 hours further cycling was carried out at 30 μA to accelerate sodiation/desodiation of the cell.

The HC in a second Na|$NaPF_6$|HC cell (cell **2**) was sodiated to 2 mV for 9 days applying a constant current of 30 μA. Achieving the low voltage plateau, the cell was kept at 2 mV for 2 days until the current reached 0 A and a capacity of ca. 220 mAh/g was achieved.

^{23}Na in-situ solid-state NMR

^{23}Na *in-situ* NMR experiments were performed on cell **1** using the same equipment and similar conditions as described in detail in the literature. [15] All experiments were conducted on a Bruker Avance III 300 MHz NMR spectrometer at 7 T corresponding to a frequency of 79.38 MHz for ^{23}Na. The spectrometer was equipped with a single channel *in-situ* probe connected to an automatic tuning and matching cycler (ATMC) as well as to an external electrochemical cycler (Bio-Logic) provided by NMR Service. This probe contains an Ag/Cu coil where the electrochemical cell was inserted and oriented perpendicular to the external magnetic field. The ATMC enables re-adjustment of the resonance circuit during the sodiation/desodiation of the cell. This re-adjustment was done by optimizing the tuning and matching capacitor positions employing a low power continuous radio wave (0.1 W) to calculate the ratio between forwarded and reflected power. On the ATM controller, low-pass filters were connected to eliminate frequencies higher than 90 MHz. Pulse lengths of 5 μs were applied in a pseudo 2D solid-echo sequence to record the ^{23} Na spectra. Each ^{23}Na *in-situ* NMR spectrum was collected with 30 000 scans using a recycle delay of 50 ms as used in the literature. [17] ^{23}Na chemical shifts were reported with respect to the signal of NaCl powder at 7.21 ppm relative to a 1 M aqueous solution of NaCl at 0 ppm.[31]

^{23}Na ex-situ solid-state NMR

General

All ^{23}Na *ex-situ* MAS NMR measurements were performed on a 600 MHz Bruker Avance III HD NMR spectrometer at 14.1 T corresponding to a frequency of 158.74 MHz for ^{23}Na. The spectra were referenced to the signal of NaCl powder at 7.21 ppm relative to 1 M aqueous solution of NaCl at 0 ppm.[31]

Cell 1

After sodiation/desodiation of cell **1** for 22 days, the galvanostatic cycling was stopped at the low-voltage plateau of 2 mV. The cell showing a capacity of ca. 160 mAh/g was disassembled in an Argon-filled glovebox. The sodiated HC electrode material was washed with dimethyl carbonate (Sigma-Aldrich), dried in vacuum, and packed to a 3.2 mm rotor under Argon atmosphere. The spectrum was recorded at 15 kHz applying a single pulse sequence with short excitation pulses of 0.2 μs length at 80 W and a repetition delay of 2.5 s. Hereby, 26 341 scans were accumulated corresponding to a measurement time of ca. 23 h to obtain an appropriate S/N ratio.

Cell 2

For further ^{23}Na *ex-situ* MAS NMR investigations cell **2** was prepared. After 11 days of sodiation to 2 mV, the Na|$NaPF_6$|HC cell exhibited a capacity of ca. 220 mAh/g. To exclude possible cause of unwanted side-reactions the cycled HC material extracted from cell **2** was not washed with dimethyl carbonate (Sigma-Aldrich). The sample was spun at 10 kHz. A single pulse sequence with excitation pulses of 3 μs length at 80 W and a recycling delay of 0.5 s was used. 200 scans were collected inca. 2 min. Subsequently, the cycled HC material was spun at 15 kHz. A single pulse sequence with excitation pulses of 3 μs length at 80 W and a recycling delay of 2.5 s were also applied. 200 scans were accumulated in ca. 10 min.

Acknowledgements

The authors thank the EU project SIMBA (Sodium-Ion and Sodium Metal Batteries for efficient and sustainable next-generation energy storage) under grant agreement number 963542 for financial support. Open Access funding enabled and organized by Projekt DEAL.

Conflict of Interests

The authors declare no conflict of interest.

Data Availability Statement

The data that support the findings of this study are available in the supplementary material of this article.

Keywords: solid-state NMR · electrochemical cells · sodium; hard carbon · in-situ characterization

[1] Z. Zhang, T. Ding, Q. Zhou, Y. Sun, M. Qu, Z. Zeng, Y. Ju, L. Li, K. Wang, F. Chi, *Renewable Sustainable Energy Rev.* **2021**, *148*, 111263.
[2] a) X. Yu, A. Manthiram, *Adv Energy Sustain Res* **2021**, *2*, 2000102; b) H. Pan, Y.-S. Hu, L. Chen, *Energy Environ. Sci.* **2013**, *6*, 2338.
[3] a) M. Wang, Q. Wang, X. Ding, Y. Wang, Y. Xin, P. Singh, F. Wu, H. Gao, *Interdiscip. Mater.* **2022**, *1*, 373–395; b) N. Yabuuchi, K. Kubota, M. Dahbi, S. Komaba, *Chem. Rev.* **2014**, *114*, 11636–11682.
[4] G. Hasegawa, K. Kanamori, N. Kannari, J. Ozaki, K. Nakanishi, T. Abe, *ChemElectroChem* **2015**, *2*, 1917–1920.
[5] Z. E. M. Reeve, C. J. Franko, K. J. Harris, H. Yadegari, X. Sun, G. R. Goward, *J. Am. Chem. Soc.* **2017**, *139*, 595–598.
[6] P. M. Bayley, N. M. Trease, C. P. Grey, *J. Am. Chem. Soc.* **2016**, *138*, 1955–1961.
[7] a) J. Górka, C. Vix-Guterl, C. Matei Ghimbeu, *C.* **2013**, *2*; b) F. Xie, Z. Xu, Z. Guo, M.-M. Titirici, *Prog. Energy* **2020**, *2*, 42002.
[8] a) S. Chen, F. Feng, Y. Yin, H. Che, X.-Z. Liao, Z.-F. Ma, *J. Power Sources* **2018**, *399*, 363–371; b) P. Liu, Y. Li, Y.-S. Hu, H. Li, L. Chen, X. Huang, *J. Mater. Chem. A* **2016**, *4*, 13046–13052; c) M. Liu, J. Zhang, S. Guo, B. Wang, Y. Shen, X. Ai, H. Yang, J. Qian, *ACS Appl. Mater. Interfaces* **2020**, *12*, 17620–17627; d) X. Zhang, C. Fan, S. Han, *J. Mater. Sci.* **2017**, *52*, 10418–10430; e) K. Vignarooban, R. Kushagra, A. Elango, P. Badami, B.-E. Mellander, X. Xu, T. G. Tucker, C. Nam, A. M. Kannan, *Int. J. Hydrogen Energy* **2016**, *41*, 2829–2846.
[9] a) S. Komaba, W. Murata, T. Ishikawa, N. Yabuuchi, T. Ozeki, T. Nakayama, A. Ogata, K. Gotoh, K. Fujiwara, *Adv. Funct. Mater.* **2011**, *21*, 3859–3867; b) A. Beda, C. Villevieille, P.-L. Taberna, P. Simon, C. Matei Ghimbeu, *J. Mater. Chem. A* **2020**, *8*, 5558–5571.

[10] H. Au, H. Alptekin, A. C. S. Jensen, E. Olsson, C. A. O'Keefe, T. Smith, M. Crespo-Ribadeneyra, T. F. Headen, C. P. Grey, Q. Cai, A. J. Drew, M.-M. Titirici, *Energy Environ. Sci.* **2020**, *13*, 3469–3479.
[11] V. Simone, A. Boulineau, A. de Geyer, D. Rouchon, L. Simonin, S. Martinet, *J. Energy Chem.* **2016**, *25*, 761–768.
[12] A. Agrawal, S. Janakiraman, K. Biswas, A. Venimadhav, S. K. Srivastava, S. Ghosh, *Electrochim. Acta* **2019**, *317*, 164–172.
[13] X. Dou, I. Hasa, M. Hekmatfar, T. Diemant, R. J. Behm, D. Buchholz, S. Passerini, *ChemSusChem* **2017**, *10*, 2668–2676.
[14] X. Dou, I. Hasa, D. Saurel, C. Vaalma, L. Wu, D. Buchholz, D. Bresser, S. Komaba, S. Passerini, *Mater. Today* **2019**, *23*, 87–104.
[15] E. Šić, M. Melzi d'Eril, K. Schutjajew, M. J. Graczyk-Zajac, H. Breitzke, R. Riedel, M. Oschatz, T. Gutmann, G. Buntkowsky, *Batteries & Supercaps* **2022**, *5*, e20220006.
[16] J. M. Stratford, A. K. Kleppe, D. S. Keeble, P. A. Chater, S. S. Meysami, C. J. Wright, J. Barker, M.-M. Titirici, P. K. Allan, C. P. Grey, *J. Am. Chem. Soc.* **2021**, *143*, 14274–14286.
[17] J. M. Stratford, P. K. Allan, O. Pecher, P. A. Chater, C. P. Grey, *Chem. Commun.* **2016**, *52*, 12430–12433.
[18] K. Gotoh, T. Yamakami, I. Nishimura, H. Kometani, H. Ando, K. Hashi, T. Shimizu, H. Ishida, *J. Mater. Chem. A* **2020**, *8*, 14472–14481.
[19] O. Pecher, P. M. Bayley, H. Liu, Z. Liu, N. M. Trease, C. P. Grey, *J. Magn. Reson.* **2016**, *265*, 200–209.
[20] J. M. Bray, C. L. Doswell, G. E. Pavlovskaya, L. Chen, B. Kishore, H. Au, H. Alptekin, E. Kendrick, M.-M. Titirici, T. Meersmann, M. M. Britton, *Nat. Commun.* **2020**, *11*, 2083.
[21] F. Poli, J. S. Kshetrimayum, L. Monconduit, M. Letellier, *Electrochem. Commun.* **2011**, *13*, 1293–1295.
[22] F. Chevallier, M. Letellier, M. Morcrette, J.-M. Tarascon, E. Frackowiak, J.-N. Rouzaud, F. Béguina, *Electrochem. Solid-State Lett.* **2003**, *6*, A225–A228.
[23] M. Thommes, K. Kaneko, A. V. Neimark, J. P. Olivier, F. Rodriguez-Reinoso, J. Rouquerol, K. S. Sing, *Pure Appl. Chem.* **2015**, *87*, 1051–1069.
[24] C. Matei Ghimbeu, J. Górka, V. Simone, L. Simonin, S. Martinet, C. Vix-Guterl, *Nano Energy* **2018**, *44*, 327–335.
[25] R. Morita, K. Gotoh, K. Kubota, S. Komaba, K. Hashi, T. Shimizu, H. Ishida, *Carbon* **2019**, *145*, 712–715.
[26] A. Sadoc, M. Body, C. Legein, M. Biswal, F. Fayon, X. Rocquefelte, F. Boucher, *Phys. Chem. Chem. Phys.* **2011**, *13*, 18539–18550.
[27] K. Gotoh, T. Ishikawa, S. Shimadzu, N. Yabuuchi, S. Komaba, K. Takeda, A. Goto, K. Deguchi, S. Ohki, K. Hashi, T. Shimizu, H. Ishida, *J. Power Sources* **2013**, *225*, 137–140.
[28] a) R. Alcántara, P. Lavela, G. F. Ortiz, J. L. Tirado, *Electrochem. Solid-State Lett.* **2005**, *8*, A222–A225; b) S. Alvin, D. Yoon, C. Chandra, H. S. Cahyadi, J.-H. Park, W. Chang, K. Y. Chung, J. Kim, *Carbon* **2019**, *145*, 67–81.
[29] R. Morita, K. Gotoh, M. Fukunishi, K. Kubota, S. Komaba, N. Nishimura, T. Yumura, K. Deguchi, S. Ohki, T. Shimizu, H. Ishida, *J. Mater. Chem. A* **2016**, *4*, 13183–13193.
[30] J.-B. Kim, G.-H. Lee, V. W. Lau, J. Zhang, F. Zou, M. Chen, L. Zhou, K.-W. Nam, Y.-M. Kang, *J. Phys. Chem. C* **2021**, *125*, 14559–14566.
[31] S. Hayashi, K. Hayamizu, *Bull. Chem. Soc. Jpn.* **1989**, *62*, 2429–2430.

Manuscript received: September 4, 2023
Revised manuscript received: October 13, 2023
Accepted manuscript online: October 17, 2023
Version of record online: November 17, 2023